the β, δ, γ, and α diastereoisomers, respectively. All the other forms are relatively unstable. A scheme for the isomerization reactions of these diastereoisomers is shown in Figure 6. The thermodynamics and kinetics of these reactions are the subject of a continuing study.

Infrared Spectral Studies of Ni(1,4-CTH)$(NCS)_2$ Isomers. The infrared data for the bis(thiocyanato) derivatives of these five stereoisomers are tabulated in Table V. All five isomers show ν(CN of NCS) bands in the 2010–2065-cm^{-1} region. Only one ν(CN of NCS) band is observed for [Ni(β-*rac*-1,4-CTH)$(NCS)_2$]. All the other stereoisomers show two ν(CN of NCS) bands. These results indicate that the axial sites are identical or very similar for [Ni(β-*rac*-1,4-CTH)$(NCS)_2$], while in the other isomers the two axial sites are different,[25] in agreement with the structures of these isomers given in Figure 4. The splitting of the two ν(CN of NCS) bands for [Ni(1,4-CTH)$(NCS)_2$] can be taken as measure of the degree of the difference of the axial sites of the complex. As shown in Figure 4, in [Ni(β-*meso*-1,4-CTH)$(NCS)_2$] all of the four amine protons are above the nickel(II)–four-nitrogen plane. In [Ni(γ-*meso*-1,4-CTH)$(NCS)_2$] three amine protons are above the nickel(II)–four-nitrogen plane; only one amine proton is below this plane. In [Ni(δ-*meso*-1,4-CTH)$(NCS)_2$] or [Ni(α-*meso*-1,4-CTH)$(NCS)_2$], two amine protons are above and the other two amine protons are below the nickel(II)–four-nitrogen plane. Thus we may expect the degree of the difference on the axial sites varies in the order [Ni(β-*meso*-1,4-CTH)$(NCS)_2$] > [Ni(γ-*meso*-1,4-CTH)$(NCS)_2$] > [Ni(δ-*meso*-1,4-CTH)$(NCS)_2$], [Ni(α-*meso*-1,4-CTH)$(NCS)_2$] > [Ni(β-*rac*-1,4-CTH)$(NCS)_2$]. The values of the splittings of the ν(CN of NCS) bandsof these isomers listed in Table V substantiate this expectation.

Acknowledgment. The authors are grateful to the Chemistry Research Center, National Science Council of the Republic of China, for financial support. We are grateful to Dr. Chi-Chao Wan and Yuan-Chung Hsieh for performing elemental analyses and for providing laboratory facilities.

Registry No. Ni(β-*rac*-1,4-CTH)$(ClO_4)_2$, 57427-11-9; Ni(β-*rac*-1,4-CTH)$(NCS)_2$, 89361-31-9; [Ni(α-*meso*-1,4-CTH)(acac)](ClO_4), 89278-58-0; Ni(α-*meso*-1,4-CTH)$(ClO_4)_2$, 89361-33-1; Ni(α-*meso*-1,4-CTH)$(NCS)_2$, 89394-78-5; Ni(α-*meso*-1,4-CTH)Cl_2, 89394-79-6; Ni(β-*meso*-1,4-CTH)$(ClO_4)_2$, 89361-35-3; Ni(β-*meso*-1,4-CTH)$(NCS)_2$, 89394-80-9; Ni(γ-*meso*-1,4-CTH)$(ClO_4)_2$, 89361-37-5; Ni(γ-*meso*-1,4-CTH)$(NCS)_2$, 89394-81-0; Ni(δ-*meso*-1,4-CTH)$(ClO_4)_2$, 87302-44-1; Ni(δ-*meso*-1,4-CTH)$(NCS)_2$, 89361-38-6; Ni(1,4-CT)$(ClO_4)_2$, 14875-35-5.

Supplementary Material Available: Figures 2 and 3 (^{1}H NMR spectra) (2 pages). Ordering information is given on any current masthead page.

(25) Gutmann, V. *Coord. Chem. Rev.* **1967**, *2*, 239.

Notes

Contribution from the Biophysics Division, Faculty of Pharmaceutical Sciences, Teikyo University, Sagamiko, Kanagawa 199-01, Japan

Preparation and Characterization of Low-Spin Iron(II) Porphyrin Complexes with Bis(phosphine) or Bis(phosphite) Axial Ligands

Toshie Ohya,* Hiromi Morohoshi, and Mitsuo Sato

Received July 5, 1983

Axial ligation in iron porphyrin complexes has been the subject of extensive investigations, in connection with its biological significance. Several reports have attempted to correlate Mössbauer data of hexacoordinate low-spin Fe(II) porphyrin complexes with the electronic properties of the fifth and sixth axial ligands.[1,2] In most cases, it is tacitly assumed that the nature of iron–porphyrin bonds is unaffected by changes in axial ligands, whereas the bonding situation is rather complicated in some cases. For example, Sams et al.[2] explained the apparent anomaly in Mössbauer parameters for carbonyl hemochromes by considering a cis effect or an "electron sink" capability of macrocyclic planar ligands.

We have prepared and characterized several new low-spin Fe(II) complexes, Fe(p)L_2, where p = the dianion of meso-tetraphenylporphine (TPP) or phthalocyanine (Pc) and L = trialkylphosphine (PR_3) or trialkyl phosphite ($P(OR)_3$). With these complexes having axial ligands of distinct σ- and π-bonding characteristics, a comparative Mössbauer investigation was carried out to verify such an "electron sink" capability of macrocycles. This study also offers the characterization of the electronic spectra of Fe(p)L_2.

Experimental Section

^{57}Fe(TPP)Cl was synthesized and purified following published methods.[3-5] ^{57}Fe(TPP)$(PR_3)_2$ (R = Et, *n*-Bu) was prepared by refluxing a solution of ^{57}Fe(TPP)Cl (70 mg) in PR_3 (1 mL) and dichloromethane (70 mL) under nitrogen for 1 h, reducing to a small volume by vacuum evaporation, and adding methanol. The black-purple crystals that resulted were collected and washed with methanol. ^{57}Fe(TPP)$[P(OR)_3]_2$ (R = Me, Et, *n*-Bu) was prepared similarly. Anal. Calcd for Fe(TPP)$(PBu_3)_2$: C, 76.1; H, 7.70; N, 5.22. Found: C, 76.2; H, 7.58; N, 5.23. Other ^{57}Fe(TPP)L_2 complexes also gave correct analyses.

FePc was purchased from Eastman Kodak. FePc$(PEt_3)_2$ was prepared by combining FePc (420 mg) and an excess of PEt_3 in benzene (170 mL) and stirring the suspension for 10 h. The filtered solution was then evaporated to a small volume and diethyl ether–ethanol (1:1) was added. On partial evaporation dark crystals precipitated. Recrystallization from toluene–pentane yielded dark green crystals. FePc$[P(n\text{-}Bu)_3]_2$ and FePc$[P(OEt)_3]_2$ were prepared as described.[6,7] Anal. Calcd for FePc$(PEt_3)_2$: C, 65.7; H, 5.76; N, 13.93. Found: C, 65.4; H, 5.65; N, 13.99. Other FePcL_2 complexes also gave correct analyses.

Electronic spectra were measured as dichloromethane solutions with small amounts of axial ligand to prevent dissociation and autoxidation with a Hitachi 200-10 spectrophotometer.

Mössbauer spectra were measured with an Elscint AME-30A equipped with a ^{57}Co(Rh) source. Powder samples were loaded under nitrogen into acrylic cells that were then sealed with resin. The Doppler velocity scale was calibrated with a metallic ^{57}Fe foil, the isomer shift δ is quoted relative to the centroid of the iron-foil spectrum. Estimated

(1) Sams, J. R.; Tsin, T. B. In "The Porphyrins"; Dolphin, D., Ed.; Academic Press: New York, 1979; Vol. IV, p 425.
(2) James, B. R.; Reimer, K. J.; Sams, J. R.; Tsin, T. B. *J. Chem. Soc., Chem. Commun.* **1978**, 746.
(3) Adler, A. D.; Longo, F. R.; Finarelli, J. D.; Goldmacher, J.; Assour, J.; Korsakoff, L. *J. Org. Chem.* **1967**, *32*, 476.
(4) Barnett, G. H.; Hudson, M. F.; Smith, K. M. *Tetrahedron Lett.* **1973**, 2887.
(5) Adler, A. D.; Longo, F. R.; Kampas, F.; Kim, J. *J. Inorg. Nucl. Chem.* **1970**, *32*, 2443.
(6) Sweigart, D. A. *J. Chem. Soc., Dalton Trans.* **1976**, 1476.
(7) Watkins, J. J.; Balch, A. L. *Inorg. Chem.* **1975**, *14*, 2720.

0020-1669/84/1323-1303$01.50/0

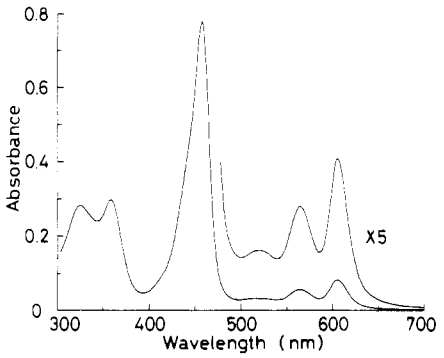

Figure 1. Electronic spectrum of $Fe(TPP)(PBu_3)_2$ in CH_2Cl_2–PBu_3 at room temperature ($[Fe(TPP)(PBu_3)_2] = 6.1 \times 10^{-6}$ M).

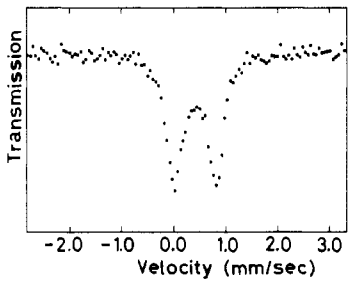

Figure 2. Mössbauer spectrum of $^{57}Fe(TPP)(PBu_3)_2$ at 3.9 K.

error limits on δ and quadrupole splitting ΔE_Q are ±0.02 mm/s.

Results and Discussion

Electronic Spectra. The $Fe(TPP)L_2$ complexes exhibited hyper spectra with "two Soret bands", one in the 445–457-nm region and the second in the near-ultraviolet (UV) 335–360-nm region. Figure 1 shows the spectrum of $Fe(TPP)(PBu_3)_2$, which has a red-shifted Soret band at 457 nm ($\epsilon = 1.277 \times 10^5$ M^{-1} cm^{-1}) and a near-UV band at 358 nm (4.88×10^4). A quite similar spectrum was obtained for $Fe(TPP)(PEt_3)_2$. In $Fe(TPP)[P(OR)_3]_2$, a red-shifted Soret band was observed at 446 nm (2.65×10^5) with a less intense band at 338 nm (3.33×10^4).

The red-shifted Soret band is a prominent optical feature observed in carbonyl cytochrome P-450. Hanson et al. presented an orbital model[8] for the origin of hyper spectra in CO–P-450 and in the CO–mercaptide model complexes and predicted that low-spin Fe(II) porphyrin complexes could exhibit hyper spectra if they have electron-donating ligands that can play the same role as the mercaptide sulfur. In our model complexes, electron-donating lone-pair σ orbitals of phosphorus atoms in the fifth and sixth positions form a symmetry orbital $a_{2u}(\sigma_5-\sigma_6)$. A phosphorus to porphyrin charge-transfer transition $a_{2u}(\sigma_5-\sigma_6) \rightarrow e_g(\pi^*)$ might then interact with the porphyrin $a_{1u}(\pi)$, $a_{2u}(\pi) \rightarrow e_g(\pi^*)$ transitions and could result in the red-shifted Soret band. The larger shift observed in $Fe(TPP)(PR_3)_2$ is consistent with such an orbital mechanism: since PR_3 is a stronger σ donor[9] than $P(OR)_3$, an orbital $a_{2u}(\sigma_5-\sigma_6)$ from PR_3 is higher in energy and the charge-transfer and the Soret transitions interact more strongly.

The complexes $FePcL_2$ exhibited spectra with an intense band in the 660–670-nm region and less intense bands in the 370–470-nm region that are distinct from those of the corresponding $Fe(TPP)L_2$ derivatives.

Mössbauer Spectra. Figure 2 shows a typical spectrum, and the Mössbauer parameters are given in Table I. The trends

Table I. Mössbauer Parameters (mm s^{-1}) for $Fe(p)L_2$ Complexes

complex	T/K	δ^a	ΔE_Q
$Fe(TPP)(PEt_3)_2$	298	0.30	0.86
	77.3	0.38	0.78
	6.1	0.40	0.82
$Fe(TPP)(PBu_3)_2$	298	0.28	0.86
	78	0.41	0.84
	6.1	0.40	0.82
	3.9	0.41	0.81
$Fe(TPP)[P(OMe)_3]_2$	298	0.26	0.46
	77.3	0.35	0.36
	6.1	0.36	0.37
$Fe(TPP)[P(OEt)_3]_2$	298	0.25	0.47
	78	0.36	0.38
	6.1	0.38	0.35
$Fe(TPP)[P(OBu)_3]_2$	298	0.26	0.48
$FePc(PEt_3)_2$	291	0.16	1.54
	78.6	0.25	1.47
$FePc(PBu_3)_2$	291	0.15	1.57
	78.8	0.24	1.47
	4.3	0.23	1.45
$FePc[P(OEt)_3]_2$	291	0.13	1.07
	78.8	0.17	0.99
	4.3	0.18	0.95

[a] Relative to metallic iron.

in δ and ΔE_Q, as p or L is varied, are summarized as follows: (a) $\delta(Fe(TPP)L_2) > \delta(FePcL_2)$, (b) $\delta(Fe(p)(PR_3)_2) > \delta(Fe(p)[P(OR)_3]_2)$, (c) $\Delta E_Q(Fe(TPP)L_2) < \Delta E_Q(FePcL_2)$, and (d) $\Delta E_Q(Fe(p)(PR_3)_2) > \Delta E_Q(Fe(p)[P(OR)_3]_2)$. These trends may provide us with some insight into the electronic structure of the iron atom in the complexes $Fe(p)L_2$. Our discussion is based on the premise that $P(OR)_3$ is a weaker σ donor and stronger π acceptor than PR_3,[9] while Pc is a stronger σ donor than TPP.[1,2,10,11]

Trends a and c parallel those found[2,10] in other axial ligand derivatives such as bis(amine) complexes. The stronger Pc $\rightarrow$ Fe(4s) σ donation compared to that of TPP $\rightarrow$ Fe(4s) leads to trend a.

For all the hexacoordinate low-spin Fe(II) complexes[14] on which magnetic perturbation Mössbauer measurements have been made, V_{zz}, the principal component of the electric field gradient (EFG), is positive and the asymmetry parameter η is nearly or exactly zero. Positive, axially symmetric EFG's are very probable to obtain in the present complexes $Fe(p)L_2$. The major contribution to the EFG comes from an imbalance of electron densities in the iron 3d orbitals.[2,11] If lattice contributions are ignored, V_{zz} is given approximately as[12]

$$V_{zz} = k[n_{x^2-y^2} - n_{z^2} + n_{xy} - \tfrac{1}{2}(n_{yz} + n_{zx})]$$

where n_i is the effective population of the appropriate 3d orbital and k is a positive constant. The larger ΔE_Q values for $FePcL_2$ (trend c) presumably reflect the stronger Pc $\rightarrow$ $Fe(3d_{x^2-y^2})$ σ donation.

Trend d, however, cannot be explained by a simple argument. In $Fe(p)[P(OR)_3]_2$ complexes, the stronger Fe $\rightarrow$ $P(OR)_3$ π back-donation causes a decrease in n_{yz} and n_{zx} and the weaker $P(OR)_3$ $\rightarrow$ Fe σ forward donation decreases n_{z^2}. Both of these effects serve to increase V_{zz} and to make ΔE_Q larger in $Fe(p)[P(OR)_3]_2$ than in $Fe(p)(PR_3)_2$. This prediction is contrary to what is observed. We therefore conclude that

(8) Hanson, L. K.; Eaton, W. A.; Sligar, S. G.; Gunsalus, I. C.; Gouterman, M.; Connell, C. R. *J. Am. Chem. Soc.* **1976**, *98*, 2672.
(9) Houghton, R. P. "Metal Complexes in Organic Chemistry"; Cambridge University Press: Cambridge, 1979.
(10) Dolphin, D.; Sams, J. R.; Tsin, T. B.; Wong, K. L. *J. Am. Chem. Soc.* **1976**, *98*, 6970.
(11) Calderazzo, F.; Frediani, S.; James, B. R.; Pampaloni, G.; Reimer, K. J.; Sams, J. R.; Serra, A. M.; Vitali, D. *Inorg. Chem.* **1982**, *21*, 2302.
(12) Bancroft, J. M.; Platt, R. H. *Adv. Inorg. Chem. Radiochem.* **1972**, *15*, 59.
(13) Kashiwagi, H.; Obara, S. *Int. J. Quantum Chem.* **1981**, 843.
(14) After our manuscript was submitted, an exceptional case $V_{zz} < 0$ was reported in a $Fe(p)(CO)_2$ complex: Reimer, K. J.; Sibley, C. A.; Sams, J. R. *J. Am. Chem. Soc.* **1983**, *105*, 5147.

replacement of axial ligands is accompanied by substantial changes in the bonding between iron and macrocyclic ligands. Upon replacement of the axial ligands PR_3 by $P(OR)_3$, there must be both an increase in p → Fe π donation to compensate for the Fe → $P(OR)_3$ back-bonding and a significant decrease in p → Fe σ donation to diminish $n_{x^2-y^2}$. This mechanism explains trend d and is consistent with trend b. The macrocyclic ligands appear to be able to modify their σ- and π-bonding characteristics to suit the requirements of the axial ligands.

Small differences in axial bond lengths might equally explain trend d as in the case for the carbonyl hemochromes.[11] Although X-ray structural data are not available for the present complexes, the electronic spectra of $Fe(TPP)L_2$ suggest the larger n_{z^2} in $Fe(TPP)(PR_3)_2$.[15] A similar situation may be expected in $FePcL_2$.

Our results support the existence of an "electron sink"[2] or an "electron buffer"[13] capability of macrocyclic ligands such as porphyrins and phthalocyanine, proposed previously. Such behavior may be responsible in part for the diverse functions in which metalloporphyrins particpate in biological systems.

Registry No. $Fe(TPP)(PEt_3)_2$, 89165-45-7; $Fe(TPP)(PBu_3)_2$, 89165-46-8; $Fe(TPP)[P(OMe)_3]_2$, 89165-47-9; $Fe(TPP)[P(OEt)_3]_2$, 89165-48-0; $Fe(TPP)[P(OBu)_3]_2$, 89165-49-1; $FePc(PEt_3)_2$, 89165-50-4; $FePc(PBu_3)_2$, 61005-30-9; $FePc[P(OEt)_3]_2$, 55925-78-5; Fe(TPP)Cl, 16456-81-8; FePc, 132-16-1.

(15) The larger red shift observed results from the stronger interaction between the phosphorus $3p_z$ and porphyrin $e_g(\pi^*)$, which suggests a stronger interaction between the phosphorus $3p_z$ and iron $3d_{z^2}$.

Contribution from the Department of Chemistry,
North Carolina State University,
Raleigh, North Carolina 27650,
and Laboratoire de Physicochimie des Solides,
Université de Nantes, 44072 Nantes Cedex, France

Characterization of the Charge Density Waves in $NbSe_3$ by Band Electronic Structure

Myung-Hwan Whangbo*[1a] and Pascal Gressier[1b]

Received July 22, 1983

$NbSe_3$ is made up of trigonal-prismatic chains that are parallel to the monoclinic *b* axis.[2] As shown by the projected view along the *b* axis in **1**, each unit cell contains three different

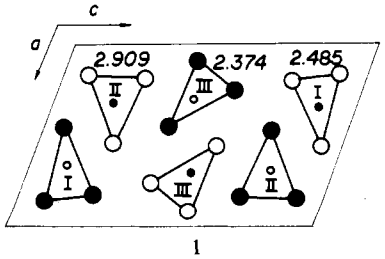

1

pairs of $NbSe_3$ chains, hereafter referred to as type I, II, and III chains. $NbSe_3$ exhibits spectacular resistivity anomalies associated with two charge density waves (CDW's).[3] The

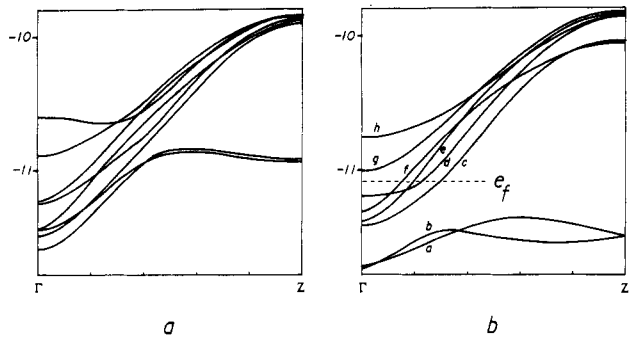

a *b*

Figure 1. d-Block band structures of $NbSe_3$ along the chain direction $\Gamma \rightarrow Z$, where Γ = (0, 0, 0) and Z = (0, 0.5, 0) in fractions of the reciprocal vectors a^*, b^*, and c^* (band orbital energies in eV): (a) for a unit cell containing six identical, ideal chains (Se–Se distances of an ideal chain taken to be the average values of the corresponding values of type I and III chains); (b) for a real unit cell **1** containing three nonequivalent pairs of chains.

Table I. Exponents ζ_μ and Valence-Shell Ionization Potential $H_{\mu\mu}$ for Slater Type Atomic Orbitals χ_μ[a,b]

χ_μ	ζ_μ	ζ_μ'	$H_{\mu\mu}$, eV
Nb 5s	1.9[c]		−10.1
Nb 5p	1.85		−6.86
Nb 4d	4.08 (0.6401)	1.64 (0.5516)	−12.1
Se 4s	2.44[d]		−20.5[e]
Se 4p	2.07		−14.4

[a] The d orbitals of Nb are given as a linear combination of two Slater type orbitals, and each is followed by the weighting coefficient in parentheses. [b] A modified Wolfsberg-Helmholz formula was used to calculate $H_{\mu\nu}$.[9] [c] Reference 10. [d] Reference 11. [e] Reference 12.

wave vectors of these CDW's are $\mathbf{q}_1$ = (0, 0.243b^*, 0) at 144 K and $\mathbf{q}_2$ = (0.5a^*, 0.263b^*, 0.5c^*) at 59 K.[4] Thus, the vector component along the chain direction (i.e., q_{1b} = 0.243b^* and q_{2b} = 0.263b^*) suggests nearly one-fourth-filled bands for both CDW's.

On the basis of the difference in the Se–Se distance (**1**), Wilson proposed an oxidation formalism of $(Nb^{5+} + 3Se^{2-})$ for type II chains.[5] Given the oxidation formalism of $(Se^{2-} + Se_2^{2-})$ for the selenium atoms of type I and II chains, therefore, there remain two d electrons per unit cell to distribute among the niobium ions of the four type I and II chains. According to this model, each type I or III chain has a nearly one-fourth-filled d-block band while each type II chain has an empty d-block band. Thus, CDW's appear only in type I and III chains, and type II chains are insulating and diamagnetic.

In order to check Wilson's model, Devreux has recently carried out a ^{93}Nb NMR study of $NbSe_3$.[6] Wilson's model led to the expectation that the NMR spectrum of $NbSe_3$

(1) (a) North Carolina State University. (b) Université de Nantes.
(2) Meerschaut, A.; Rouxel, J. *J. Less Common Met.* **1975**, *39*, 197.

(3) Chaussy, J.; Haen, P.; Lasjaunias, J. C.; Monceau, P.; Waysand, G.; Waintal, A.; Meerschaut, A.; Molinié, P.; Rouxel, J. *Solid State Commun.* **1976**, *20*, 759. (b) Monceau, P.; Ong, N. P.; Portis, A. M.; Meerschaut, A.; Rouxel, J. *Phys. Rev. Lett.* **1976**, *37*, 602. (c) Ong, N. P.; Monceau, P. *Phys. Rev. B: Solid State* **1977**, *16*, 3443. (d) Grüner, G.; Tippie, L. C.; Sanny, J.; Clark, W. C.; Ong, N. P. *Phys. Rev. Lett.* **1980**, *45*, 935. (e) Fleming, R. M.; Grimes, C. C. *Phys. Rev. Lett.* **1979**, *42*, 1923. Gill, J. C. *J. Phys. F* **1980**, *10*, 281. (g) Monceau, P.; Richard, J.; Renard, M. *Phys. Rev. B: Condens. Matter* **1982**, *25*, 931. (h) Richard, J.; Monceau, P.; Renard, M. *Phys. Rev. B: Condens. Matter* **1982**, *25*, 948. (i) Monceau, P.; Richard, J.; Renard, M. *Phys. Rev. Lett.* **1980**, *45*, 43. (j) Weger, M.; Grüner, G.; Clark, W. C. *Solid State Commun.* **1980**, *35*, 243.
(4) (a) Hodeau, J. L.; Marezio, M.; Roucau, C.; Ayroles, R.; Meerschaut, A.; Rouxel, J.; Monceau, P. *J. Phys. C* **1978**, *11*, 4117. (b) Tsutsumi, K.; Tugagaki, T.; Yamamoto, M.; Shiozaki, Y.; Ido, M.; Sambongi, T.; Yamaya, K.; Abe, Y. *Phys. Rev. Lett.* **1977**, *39*, 1675. (c) Fleming, R. M.; Moncton, D. E.; McWhan, D. B. *Phys. Rev. B: Condens. Matter* **1978**, *18*, 5560.
(5) Wilson, J. A. *Phys. Rev. B: Condens. Matter* **1979**, *19*, 6456.

0020-1669/84/1323-1305$01.50/0